

Published in final edited form as:

J Hazard Mater. 2017 January 15; 322(Pt A): 301–309. doi:10.1016/j.jhazmat.2016.04.015.

***Chironomus riparius* exposure to fullerene-contaminated sediment results in oxidative stress and may impact life cycle parameters**

G.C Waissi^{†,*}, S Bold[§], K Pakarinen[†], J Akkanen[†], M.T Leppänen[‡], E.J Petersen[¶], and J.V.K Kukkonen^{||}

[†]Department of Biology, University of Eastern Finland, Joensuu, Finland [§]GEOMAR Helmholtz Centre of Ocean for Research Kiel, Germany [‡]Finnish Environment Institute, Jyväskylä, Finland [¶]Material Measurement Laboratory, National Institute of Standards and Technology, Gaithersburg, MD USA ^{||}University of Jyväskylä, Department of Biological and Environmental Science, Jyväskylä, Finland

Abstract

A key component of understanding the potential environmental risks of fullerenes (C_{60}) is their potential effects on benthic invertebrates. Using the sediment dwelling invertebrate *Chironomus riparius* we explored the effects of acute (12 h and 24 h) and chronic (10 d, 15 d, and 28 d) exposures of sediment associated fullerenes. The aims of this study were to assess the impact of exposure to C_{60} in the sediment top layer ((0.025, 0.18 and 0.48) C_{60} mg/cm²) on larval growth, oxidative stress and emergence rates and to quantify larval body burdens in similarly exposed organisms. Oxidative stress localization was observed in the tissues next to the microvilli and exoskeleton through a method for identifying oxidative stress reactions generated by reactive oxygen species. Rapid intake of fullerenes was shown in acute experiments, whereas body residues decreased after chronic exposure. Transmission electron microscopy analysis revealed oxidative damage and structural changes in cells located between the lipid droplets and next to the microvilli layer in fullerene exposed samples. Fullerene associated sediments also caused changes in the emergence rate of males and females, suggesting that the cellular interactions described above or other effects from the fullerenes may influence reproduction rates.

Keywords

Carbon nanoparticle; Ecotoxicology; Chironomidae

1. Introduction

The increased use of carbon nanoparticles, e.g. fullerenes (C_{60}), leads to their continued release into the environment. Some applications of fullerene enabled products, such as

*Correspondence may be addressed to (greta.waissi @uef.fi, +358503230436).

cosmetics, provide a direct route to aquatic ecosystems via waste water treatment plants [1]. In the aquatic ecosystems, fullerenes may accumulate in surface sediments [2, 3] exposing benthic invertebrates.

The methods to test for the potential ecotoxicological effects of nanomaterials are still under development. While several studies have suggested that standard tests, such as those developed by the Organization of Economic Cooperation and Development (OECD), can be used for nanoparticle testing with modifications[4, 5], the exact modifications needed for those tests are unclear. In a recent review of OECD test methods for nanoparticle ecotoxicity testing, the appropriate method for spiking sediments with nanoparticles was recognized as a key topic for additional research [6]. Two relevant spiking approaches are mixing nanoparticles directly with the sediment, the method traditionally used to spike sediments with dissolved chemicals, or allowing the particles to settle onto the sediment from the overlying water, forming a layer of particles on the surface. It has been suggested though that different nanoparticle exposure methods lead to different response mechanisms by the benthic invertebrate *Chironomus riparius* larvae [7, 8]. In addition, it may be more appropriate to relate nanoparticle effects in complex matrices, such as sediments where quantification of the nanomaterial concentration may be challenging, to the body burden inside the organism instead of the concentration in the sediment [6].

The possible toxicological effects of fullerenes C₆₀ have been demonstrated in our previous study [7] in which we observed decreased growth by *C. riparius* and areas with damaged microvilli in the digestive system when larvae were exposed to C₆₀ in the top layer of the sediment. However, the body burden was not quantified. In addition, exposure to fullerenes in sediments spiked by mixing the fullerenes directly with the sediment have been shown to negatively impact *C. riparius* larval growth and development rates even at relatively low fullerene concentrations[8]. A subtle change in the emergence period for males and females was observed which could influence the local species population; because adult midges have a life span of only a few days, there needs to be a several day overlap after both the male and female flies have emerged for reproduction to occur. The underlying mechanisms of these effects are unclear but could be caused by chemical or physical impacts of the fullerenes on the gut tract and surrounding tissues.

Formation of reactive oxygen species (ROS) is known to damage and degrade lipids, proteins and DNA thus changing the structure and function of the cell and potentially leading to cell death [9, 10]. While exposure to nano-TiO₂ increased antioxidant enzyme activities in *Daphnia magna*, necrotic changes conceivably caused by oxidative stress in alimentary canal cells in this organism have also been reported [11]. In addition, exposure of *C. riparius* to silver nanoparticles in sediments caused changes in the gene-expression of glutathione S-transferases indicating oxidative stress [12].

In this study *C. riparius* larvae were exposed to fullerene (C₆₀) using the environmentally realistic method of allowing the fullerenes to settle down on the sediment surface from the overlying water [7]. Quantitative measurements of C₆₀ body burdens in *C. riparius* after exposure to three fullerene concentrations were compared to several toxicological endpoints to assess potential acute and chronic effects: larval mortality and growth, emergence time,

mass of adult midges, and localized oxidative stress in the organism cells. Testing higher fullerene concentrations enabled the comparison between body burden concentrations and results from these endpoints, while lower concentrations would have yielded chronic exposure body burdens below the limit of detection with our analytical method. This study provides the first data on the localization of oxidative damage in tissues in benthic invertebrates after carbon nanoparticles exposure.

2. Experimental methods

2.1 Preparation and characterization of the experimental sediments

Crystalline fullerene (C₆₀) powder (purity 98 %) (Sigma-Aldrich, USA) was added to 2 L of artificial fresh water (prepared by adding inorganic salts MgSO₄*7 H₂O (24.7 mg/L), CaCl₂*H₂O (58.8 mg/L), KCl (1.2 mg/L) and NaHCO₃ (13.0 mg/L), to MilliQ water, > 18.2 mΩ, Ca+Mg hardness 0.5 mmol/L) [13, 14]. The fullerene powder was previously analyzed for metal traces using inductively coupled plasma optical emission spectrometry (ICP-OES, IRIS Intrepid II XSP) measurements [8] (Supplemental Material Table S1). The C₆₀ suspension was stirred for two weeks at 1000 rpm (105 rad/s) by a magnetic stirrer [15–17]. The C₆₀ concentration of suspensions was measured before the experiments [13] at a wavelength of 335 nm [18] by using spectrophotometric measurements (ultraviolet (UV)/vis spectrophotometer, Cary 50BIO mulgrave, Australia). The absorbance at 335 nm was compared to the calibration curve documented in our previous paper [8].

The OECD method [19] for preparing artificial sediment was utilized in this study. The sediment was prepared by mixing 20 % of kaolinite clay, 75 % of quartz sand (50 % of the particles in the range of 50 to 200 μm), and 5 % of peat powder (*Sphagnum* sp.) (all percentages are on a dry mass basis) and then adjusting the pH to 7.0 with CaCO₃. Based on the results of our previous studies [7, 8], 0.5 % *Urtica* sp. dw (particle size <0.5 mm) were used as a food source. *Urtica* was added in each treatment before the beginning of the experiment. The dry mass of the sediment was 63 % to 70 % and the measured total organic carbon content (TOC) ranged from 2.51 g/kg to 2.72 g/kg (Multi N/C 2100 Analytic Jena AG Germany).

Fullerene particle sizes were characterized by transmission electron microscopy (TEM) (Zeiss 900, West Germany, 50 kV incident beam energy) using the same method as in our previous studies [7, 8]. In brief, the suspension was diluted (1:30 volumetric dilution) with artificial freshwater, and 8 μL of the diluted sample was added to a Formvar (SPI supplies US) polyvinyl resin-coated 150-mesh copper grid (Leica Wetzlar Germany). The grids were air dried for one hour, after which they were placed into a desiccator overnight prior to TEM analysis (magnification range 3 kx to 85 kx). The largest dimension of the fullerene agglomerates was used for the size distribution analysis.

2.2 Test organisms

C. riparius were cultured in the laboratory of the University of Eastern Finland. Their treatment and hatching was conducted similarly as in our previous study [7] with a 16:8 h light:dark period. Acute experiments started with fourth instar larvae (10 d post hatch).

Chronic experiments started with first instar larvae (3 d post hatch) as instructed in OECD test guideline 218 [20]. Starting the acute experiment with older larva (10 d post hatch) compared to the chronic experiments was necessary to have a sufficient organism mass for the extractions and because the organisms would be at a similar age and size at the end of both experiments. All midges were exposed individually in 50 ml glass containers with a surface area of 9.6 cm².

2.3 Exposure procedure

A modified version of the OECD standard method 218 [20] was used to create the exposure conditions. Ten g of artificial sediment were added to 50 mL glass beakers and then different volumes of a fullerene suspension were added to the overlying water and allowed to settle for two days, creating thin layers on the top of the sediment with different fullerene loadings (treatments A, B, and C; average surface densities of C₆₀ on the sediment surface in different experiments are shown in Table 1). Concentrations selected here were based on our previous findings [7] where the exposure concentration, similar to treatment C in this study, caused an adverse effect to *C. riparius* growth and based on using the lowest possible concentration which still formed a complete C₆₀ layer on the sediment surface. This exposure approach causes *C. riparius* larvae to be directly exposed to C₆₀ since they ingest particles from the sediment surface as a food source. After two days, the C₆₀ suspension was removed and carefully replaced with 40 mL of artificial freshwater for treatments B and C. However, the suspension was not removed from the beakers for treatment A, because the volume added was sufficiently small (2 mL) that it could not be removed without causing disturbing the C₆₀ layer on the sediment surface; the concentration of C₆₀ on the surface of these beakers was determined by measuring samples from the C₆₀ stock suspension and assuming that 100 % of the added C₆₀ formed the surface layer. After allowing the beakers to set for 1 d to ensure a stable layer of C₆₀ on top of the sediment, aeration was started. Overnight, one larva was carefully added below the water surface with a Pasteur pipette to each beaker while the aeration was stopped for few hours; the number of larvae tested per experiment is provided in Table S2. Water quality parameters in the overlying water were tested at the beginning and at the end of the experiments and were shown to be within the suitable range for the larvae [20]. Additional details are provided in the Supplemental Material.

Organisms were exposed individually to exclude the possible effects of higher larval density on growth and mortality [21]. UV/Vis spectrophotometry was used to measure the mass of C₆₀ that settled on top of the sediment prior to larvae addition using the method described in our previous study [7]. Briefly, 200 µL of overlying water was sampled and mixed with 200 µl 2% NaCl solution and 2 mL toluene. The mixture was vortexed and sonicated for 10 min in a bath sonicator (Sonorex Super RK 106; Bandelin).

Fullerenes were extracted from *C. riparius* larvae by using a method previously reported for *D. magna* [13] and *Lumbriculus variegatus* [2] and analyzed using a spectrophotometric measurement described in the Supplemental Material. Gut tract and histological changes were observed with TEM. Because results of a previous study showed decreased growth when exposing larvae to the highest fullerene concentration in this study (treatment C)[7],

the effect of only the two lower fullerene treatments (treatments A and B) were analyzed in 10 d growth experiments.

2.4 Experimental setup

2.4.1. Extraction experiments and procedure—Body burdens of seven larvae were measured in each treatment after acute (12 h and 24 h) and chronic (10 d and 15 d) exposures. For acute exposures, larvae were first grown in unamended (i.e., without C₆₀) artificial sediment to the fourth and final instar stage. Then, the larvae were carefully moved to exposure beakers containing treatments A, B, or C (see Table 1 for exposure concentrations). Larvae were exposed to fullerenes for 12 h and 24 h. Controls without fullerenes were handled similarly. Chronic experiments started with first instar stage larvae (3 d post hatch) and lasted for 10 d or 15 d. Depuration was tested for treatments B and C by conducting a 10 d chronic exposure with first instar stage larvae and then moving the organisms to depurate in sediment without fullerenes for 4 d.

2.4.2 Localization of ROS—Reactive oxygen species (ROS) react either spontaneously with other molecules or are catalyzed by the enzyme superoxide dismutase to form H₂O₂. We used a method to determine the distribution of hydrogen peroxide in the *C. riparius* tissues. This approach is based on the formation of a water-insoluble electron-dense precipitate of cerium perhydroxide (Ce(OH)₂OOH), which can be detected by TEM [22] after addition of cerium chloride to thin sections and the reaction of the cerium chloride with hydrogen peroxide present in the tissues. The advantage of this approach over measuring biomarkers of oxidative stress in whole organisms is that it allows for the precise localization of H₂O₂ production in the organism tissue [23]. A detailed description of this method is provided in the Supplemental Material.

2.4.3. Larval development; growth and emergence experiments—Larval growth rates were determined in a separate experiment. Larvae were exposed to different concentrations of fullerenes (treatments A and B; treatment C was tested for this endpoint in a previous study [7]) for 10 d. At day 10, larvae were sieved out from the sediment (Ø 200-µm sieve), counted and preserved in ethanol (94 %). Afterwards, they were analysed using a stereomicroscope (Nikon SMS 800) to measure body length, head capsule length and width. After heating at 100 °C until no further mass change occurred, larvae dry masses were measured using a microbalance (Sartorius 4503 micro).

Larval development to adult midges was investigated through performing an emergence experiment using the same C₆₀ concentration treatments (A, B, and C) as in the uptake experiments. It is expected that changes in the larval growth rate [7] might be reflected in a shorter emergence time or the organisms failing to emerge [21]. After the first 10 d, larvae were fed three times a week with TetraMin-suspension (0.12 mg/larva/d) by stopping aeration and adding the TetraMin-suspension gently to the sediment surface [7]. To prevent adult midges from escaping, nets were placed above the containers and midges were collected daily, counted and their dry masses (the adults were heated at 40 °C until no further mass changes occurred) were measured using a microbalance.

2.5. Calculation and statistics

Data was analysed using GraphPad Prism 5 (Graphpad software) and SPSS 19 for Windows. The normality of the data was tested with the Shapiro-Wilk test for normality. If the data was normally distributed, one-way analysis of variance (ANOVA) followed by Dunnett's multiple comparison post-hoc test was performed. If data was not normally distributed, the Kruskal-Wallis test followed by Dunn's multiple comparison post-hoc test was used. Results were indicated as being significantly different if $P < 0.05$. The emergence data was analysed by comparing survival curves using the Log-rank (Mantel-Cox) test.

3. Results

3.1 Characterization of aqueous C₆₀ suspensions

According to the TEM images (Supplemental Material Fig. S1) made from the stock suspensions for the acute, chronic, growth and emergence experiments, C₆₀ agglomerates had average sizes of (1166 ± 1185 , 925 ± 2099 , 465 ± 314 and 1087 ± 1052) nm, respectively ($n = 200$ for each experiment; uncertainties hereafter indicate standard deviation values). The agglomerates were heterogeneous in size, consisting of size ranges up to 7693 nm and had large standard deviations. Three fullerene suspensions (acute, chronic and emergence) contained over 19 % of large particles (> 1000 nm), a portion which most likely would settle down on the sediment. In the fullerene suspension used in the chronic and growth exposure, particles sized 100 nm to 300 nm were most frequent (Supplemental Material Fig. S1). Agglomerates were observed to be roughly spherical or cubical in form, a result similar to those in our previous studies [7, 8].

3.2. Larval body residues

Body residues were highest after 12 h of exposure, indicating rapid uptake of fullerenes, and decreased in all treatments after 24 h (Fig. 1); one dead larvae in treatment A for the 12 h and 24 time points and dead larvae observed in other treatments (two dead larvae in Treatment B for the 10 d and 15 d time points, and for treatment C, two after 10 d and one after 15 d of exposure) were excluded from determination of the average body burden values. Table 2 summarizes the uptake and development data from all experiments. While the C₆₀ concentrations in treatment A were similar after 12 h and 24 h, the difference between the two time points increased with greater fullerene concentrations in treatments B and C (Fig. 1A).

A comparison between the body burden results from the acute and chronic exposure conditions showed that the highest C₆₀ tissue concentrations were measured after 12 h and decreased with longer exposure durations. This can be clearly seen in a comparison among time points for treatment C (Fig. 1A–B). After 10 d (chronic exposures), the concentrations in all organisms for treatment A were below the detection limit (10 ng C₆₀/mg wet mass). Similarly, concentrations over the detection limit could be measured in only two samples from treatment A after exposure for 15 d; all organisms without detectable fullerene concentrations were excluded for the calculation of the average body burden values. The C₆₀ concentrations ranged from (0.46 ± 0.25) $\mu\text{g C}_{60}/\text{mg wet mass}$ in treatment B to (0.69 ± 0.31) $\mu\text{g C}_{60}/\text{mg wet mass}$ in treatment C after 10 d. However, two larvae in both

treatments were under the detection limit, and one of the larvae was also dead for treatment B. Overall, the body burdens increased with higher fullerene loadings in the sediment for each time point. A 4 d fullerene depuration experiment after a 10 d chronic exposure revealed a decrease in the body burdens to $(0.0072 \pm 0.0065) \mu\text{g C}_{60}/\text{mg wet mass}$ and $(0.0079 \pm 0.0032) \mu\text{g C}_{60}/\text{mg wet mass}$ for treatments B and C, respectively; values for only three of the larvae were above the detection limit for each treatment. The percentage decrease for both treatments was $\approx 99\%$, a value substantially greater than the increase in the average organism mass during this period (64 % on average) indicating that the change cannot be explained solely by organism growth.

3.4. Cell imaging and signs of oxidative stress

TEM imaging revealed that the guts of the exposed larvae were fully packed with C_{60} agglomerates in both the acute and chronic exposures. TEM images showed black aggregates in the exposed samples which were not observed at such high quantities in the control organisms (Supplementary Material Fig. S2A–F). Evaluation of the control organism tissues revealed nuclei in cells next to the microvilli and the exoskeleton layers after 12 h (Supplemental Material Fig.S2A) and after 10 d of treatments (Supplemental Material Fig.S2E) and mitochondria as well (Supplemental Material Fig.S2B and 2F). The microvilli layer was clearly observed (Fig. 2D) as was the structure of the tissue next to this layer.

Control organisms had fewer precipitates (Supplemental Material Fig.S2 A–F) compared to all other treatments (Supplemental Material Figures S3, S4, and S5), and had no precipitates distally from the microvilli layer (Supplemental Material Fig.S2 D). However, some precipitates were observed in the control organisms (Supplemental Material Fig. S 2 C) which is caused by normal oxidative reactions [24]. The positive control test organisms revealed changes localized precipitates in tissues, indicative of oxidative stress (Supplemental Material Fig. S3A–F). In addition, lipid droplet formation was increased (Supplemental Material Fig. S3D), which is a feature of oxidative stress [25]. The tissue next to the microvilli layer showed large precipitates after chronic exposure (Supplemental Material Fig. S3A, C, E, and F) which were close to lipid droplets (Supplemental Material Fig. S3E). These observations were mainly detected after the chronic exposure, whereas after acute exposure the frequency of precipitates was lower.

Histological changes occurred in the nucleus and mitochondrial structures in the fullerene treatments (Fig. 2B and C, Supplemental Material Fig. S4A, C, E and Fig. S5A, C, E). The precipitated cerium perhydroxides could be detected by TEM in exposed samples after 12 h and 10 d of exposure in all treatments (Fig. 2 and Supplemental Material Fig. S4, S5). The frequency of precipitates was higher after chronic exposure, a result similar to that found with the positive control. After 10 d of exposure in treatment B, numerous precipitates were observable in the tissue (Supplemental Material Fig. S4E and F) and large precipitates occurred close to lipid droplets (Supplemental Material Fig. S4D). Similarly, in treatment C, precipitates were detected after chronic exposure (Supplemental Material Fig. S5) and histological changes were observable in the structures of the nuclei and mitochondria (Supplemental Material Fig. S5A, C, D, E, and F). Fewer precipitates were observed for treatment C after an acute experiment compared to the other treatments.

In treatment A, larger precipitates were observed after 10 d (Fig. 2) whereas some precipitate formations were detected after 12 h. Those precipitates were most abundant between the lipid droplets or close to them (Fig. 2A, D, E, and F). Precipitates were also detected next to the microvilli layer in the alimentary canal cells and in the tissue next to the exoskeleton. In addition, the loss of mitochondrial ultrastructure was localized distally from the microvilli layer (Fig. 2B and C and Supplemental Material Fig. S4A and C).

3.5. Larval development: growth and emergence

Larval growth, dry mass, and average body length were not significantly affected in treatments A or B (Table 2 and Supplementary Material Fig. S6 and Table S3). All larvae in treatment A were in their final instar stage, whereas in treatment B one larva did not reach the final instar stage. Dry masses of the adults did not differ significantly (Supplementary Material Fig. S8). Also, one larva in the third instar stage was found in the control treatment (Supplemental Material Fig. S7).

The emergence of the adults occurred modestly earlier in fullerene treatments (Table 2) although a significant difference was found only in treatment A (Fig. 3 A). Analyzing results after combining all fullerene treatments showed that there was not a significant difference compared to the control (Fig. 3 B) indicating that the emergence rate is not evidently affected by the fullerene exposures.

The males exposed to fullerenes consistently emerged more quickly than those in the control organisms, and the result showed a slight dose-dependent behaviour (Fig. 4). Females exposed to fullerenes emerged statistically faster compared to the controls only for treatment A, the lowest fullerene concentration; a dose-dependent response was not observed.

Although the cumulative emergence in treatment B and C did not differ compared to the controls a trend affecting population dynamic can be seen (Fig. 4). In those treatments, males tend to emerge faster and within a shorter time period compared to the controls (Fig. 4 inserted Figure). Particularly, in treatment C there was a significant difference in the male emergence times (* $p < 0.005$) and the time of emergence between males and females did not overlap (Fig. 4).

4. Discussion

4.1 Body residues

Fullerene agglomerates taken up by the benthic invertebrate *C. riparius* could be accurately extracted with toluene (Supplemental Material Fig. S2). Fullerene body burdens, measured for the first time here for *C. riparius*, decreased with longer exposure periods and followed a dose-dependent behavior. It is unlikely that the lower body burdens after prolonged exposure is a result of fullerene biodegradation, because previous studies have not observed degradation of fullerenes [26, 27]; similar results have been observed for other carbon nanomaterials [28] although a specific microbial consortium which was able to biodegrade multiwall carbon nanotubes [29]. The decreased concentrations after longer exposure could be a result of organisms decreasing their feeding when getting close to the pupal stage or that larvae are able to depurate fullerenes. In another study with benthic oligochaete *L.*

variegatus, fullerene uptake was detected after 28 d and the size of C₆₀ in sediments was observed to impact the uptake rate [30]. The body burdens were also much lower in *L. variegatus* compared *C. riparius* body burdens found in this study. The cause of the difference was unclear but could be from difference between the species, concentrations, or spiking methods. Previous studies have shown fullerene packing in the gut tracts of *D. magna*, *L. variegatus*, and *C. riparius*[2, 7, 13], and TEM analysis in this study also did not indicate absorption of fullerenes across the gut tract in *C. riparius*. Thus, the body burdens measured in this study differ from bioaccumulation of hydrophobic organic chemicals which are absorbed into systemic circulation in the organisms[31, 32]. The finding that fullerenes accumulate in *C. riparius* quite rapidly accords with previous studies with *Daphnia magna* [13] and studies with *D. magna* accumulation of other carbon nanomaterials [14, 33, 34].

4.2 Cell imaging and localization of oxidative stress in cells

As expected, the positive control samples with cadmium affected the cell nucleus given that ROS can damage the DNA and membranes, potentially leading to cell death [24]. Sufficient oxidative stress can lead to apoptosis which can be seen in cells by the following features: cell shrinkage, chromatin condensation, cell surface blebbing, chromatin migration to the nuclear margins, nuclear fragmentation and the formation of several membrane-bound apoptotic bodies [35, 36]. Some of these features were evident in the cells of organisms exposed to fullerenes, in addition to the positive control samples, suggesting that apoptosis may have occurred in some cells. In addition, fullerene exposed organisms and positive control organisms also showed a number of changes compared to the control organisms: a higher frequency of lipid droplet formation (a sign under oxidative stress conditions [25]) nucleus shrinkage, and changes to the mitochondria (swollen mitochondria, rupture of mitochondrial membranes, and a decrease in mitochondrial matrix density). Identification of cerium in tissues by energy dispersive spectroscopy was inconclusive because cerium has more than one characteristic peak over the spectrum and this peak seems to overlap with peaks from other elements more abundant in the sample such as carbon, oxygen, copper (originating from the grids) or osmium (used in the post fixation process). Thus, observations from generated ROS-species were based on identifying clear precipitates which were not as abundant in the control samples. It is interesting to note that the markers of oxidative stress were greater after exposure for 10 d compared to 12 h even though the body burdens were smaller after 10 d. The cause of this finding is unclear but seems to indicate that prolonged exposure to the fullerenes caused more oxidative stress than acute exposure with a higher body burden. Oxidative stress initiated by some stressor is largely dependent on the formation of reactive oxygen species. Once initiated this process can be self-sustaining and goes on without the original stressor [37, 38]. Additional research is needed to better understand the relationship between fullerene body burdens, exposure duration, and oxidative stress.

4.3 Growth and emergence rate

The development time for both males and females was normal with males emerging earlier [21, 39, 40]. However, this study revealed slightly faster emergence rate in the lowest treatment A (0.028 mg/cm²), but no changes in treatments B and C or when all of the data from the fullerene treatments were combined. The cause of the change in the emergence

time at only the lowest treatment is unclear, but there does seem to be an overall but not statistically significant trend toward earlier emergence times. A shifted emergence time has also been observed with metal nanoparticles [41] as well as with fullerenes with lower doses concentrations around 0.5 mg C₆₀/kg sediment dry mass [8]. Importantly, there were several days between the distribution of emergence times for the males and females for treatment C which could lead to a situation where breeding is impaired given their short life span (approximately 5 d to 7 d).

Overall, some similar trends were observed when comparing the two different fullerene spiking methods. For example, the growth rates were not decreased for the concentrations tested in this study using the fullerene settling method which is similar to findings in the previous study with direct mixing at concentrations of 40 mg/kg and 60 mg/kg. However, direct mixing with the 80 mg/kg concentration did have an effect on the growth rate as did treatment C in our previous study [7, 8]. As previously described, the two spiking approaches were also similar in that clear dose-response trends were not observed across the fullerene concentrations tested for the growth rate endpoint and that earlier emergence was also observed for higher fullerene concentrations with the direct spiking method.

Nevertheless, there are several challenges related to the fullerene settling exposure method. First, a high concentration of fullerene needs to settle to the sediment surface to form a layer of fullerene particles. If the lowest concentration tested in this study was converted to a concentration in terms of mg/kg of sediment, it would be several orders of magnitude higher than the highest concentration used in the previous study in which the fullerenes were directly spiked to the sediment. It was necessary to use this high of a concentration because a lower concentration may not form a complete fullerene layer on the sediment surface. If a lower concentration of fullerenes was present on the sediment surface after settling, it is possible that the settled fullerenes would get mixed into the sediment when the overlaying water was added thus forming a condition analogous to that in the direct spiking method. In addition, it is possible that the concentration of fullerenes in the suspension in the overlying water used to form the fullerene layer would impact the results because it could impact the size distribution of the fullerene agglomerates on the surface. Using too low of a fullerene concentration in the overlying water could result in a lack of settling thus hindering preparing lower fullerene exposure concentrations. Thus, producing a fullerene concentration range spanning several orders of magnitude in which the only parameter that varies is the fullerene concentration on the sediment surface could be highly challenging with the settling method.

5. Conclusion

This study revealed several key findings: rapid uptake of fullerenes by *C. riparius*, impact of fullerenes on certain endpoints such as the emergence rate of males and females, and the generation of oxidative stress. Signs of oxidative stress, identified as a formation of precipitates in tissues and from the increased formation of lipid droplets, occurred next to the microvilli layer and in alimentary canal cells. Importantly, the results generated in this study enabled a comparison between the fullerene body burdens and multiple endpoints and between toxicological impacts observed for the two fullerene spiking methods.

Supplementary Material

Refer to Web version on PubMed Central for supplementary material.

Acknowledgments

This research was funded by the Finnish Graduate School in Environmental Science, Technology (EnSTe) and by Academy of Finland project 214545 and Olvi Foundation. We thank Marja Noponen and Anna-Liisa Karttunen for preparing the TEM samples, Jari Leskinen and Arto Koistinen from BioMater Center for technical help with TEM imaging, and Youlia Yourchenko for her assistance in the laboratory experiment. Certain commercial equipment, instruments and materials are identified in order to specify experimental procedures as completely as possible. In no case does such identification imply a recommendation or endorsement by the National Institute of Standards and Technology nor does it imply that any of the materials, instruments or equipment identified are necessarily the best available for the purpose.

References

1. Morris, J. Willis, Environmental Protection Agency Nanotechnology White Paper, Science Policy Council. Washington. USA: U.S. Environmental Protection Agency; 2007.
2. Pakarinen K, Petersen EJ, Leppänen MT, Akkanen J, Kukkonen JVK. Adverse effects of fullerenes (nC60) spiked to sediments on *Lumbricus variegatus* (Oligochaeta). *Environmental Pollution*. 2011; 159:3750–3756. [PubMed: 21852027]
3. Pakarinen K, Petersen EJ, Alvila L, Waissi-Leinonen GC, Akkanen J, Leppänen MT, Kukkonen JVK. A screening study on the fate of fullerenes (nC60) and their toxic implications in natural freshwaters. *Environ. Toxicol. Chem.* 2013; 32:1224–1232. [PubMed: 23404765]
4. Handy RD, Cornelis G, Fernandes T, Tsyusko O, Decho A, Sabo-Attwood T, Metcalfe C, Stevens JA, Klaine SJ, Koelmans AA, Horne N. Ecotoxicity test methods for engineered nanomaterials: practical experiences and recommendations from the bench. *Environ. Toxicol. Chem.* 2012; 31:15–31. [PubMed: 22002667]
5. Kuehnelt D, Nickel C. The OECD expert meeting on ecotoxicology and environmental fate - Towards the development of improved OECD guidelines for the testing of nanomaterials. *Sci. Total Environ.* 2014; 472:347–353. [PubMed: 24461369]
6. Petersen EJ, Diamond S, Kennedy AJ, Goss G, Ho K, Lead JR, Hanna SK, Hartmann N, Hund-Rinke K, Mader B, Manier N, Pandard P, Salinas ER, Sayre P. Adapting OECD Aquatic Toxicity Tests for Use with Manufactured Nanomaterials: Key Issues and Consensus Recommendations. *Environmental science & technology*. 2015; 49:9532–9547. [PubMed: 26182079]
7. Waissi-Leinonen GC, Petersen EJ, Pakarinen K, Akkanen J, Leppänen MT, Kukkonen JVK. Toxicity of fullerene (C60) to sediment-dwelling invertebrate *Chironomus riparius* larvae. *Environmental Toxicology and Chemistry*. 2012; 31:2108–2116. [PubMed: 22740114]
8. Waissi-Leinonen GC, Nybom I, Pakarinen K, Akkanen J, Leppänen MT, Kukkonen JVK. Fullerenes(nC60) affect the growth and development of the sediment-dwelling invertebrate *Chironomus riparius* larvae. *Environmental Pollution*. 2015; 206:17–23. [PubMed: 26142746]
9. Petersen EJ, Tu X, Dizdaroglu M, Zheng M, Nelson BC. Protective Roles of Single-Wall Carbon Nanotubes in Ultrasonication-Induced DNA Base Damage. *Small*. 2013; 9:205–208. [PubMed: 22987483]
10. Petersen EJ, Reipa V, Watson SS, Stanley DL, Rabb SA, Nelson BC. DNA Damaging Potential of Photoactivated P25 Titanium Dioxide Nanoparticles. *Chem. Res. Toxicol.* 2014; 27:1877–1884. [PubMed: 25162377]
11. Kim KT, Klaine SJ, Cho J, Kim S, Kim SD. Oxidative stress responses of *Daphnia magna* exposed to TiO₂ nanoparticles according to size fraction. *Sci. Total Environ.* 2010; 408:2268–2272. [PubMed: 20153877]
12. Nair PMG, Park SY, Lee S, Choi J. Differential expression of ribosomal protein gene, gonadotrophin releasing hormone gene and Balbiani ring protein gene in silver nanoparticles exposed *Chironomus riparius*. *Aquatic Toxicology*. 2011; 101:31–37. [PubMed: 20870301]

13. Tervonen K, Waissi G, Petersen EJ, Akkanen J, Kukkonen JVK. Analysis of Fullerene-C-60 and Kinetic Measurements for its Accumulation and Depuration in *Daphnia Magna*. *Environmental Toxicology and Chemistry*. 2010; 29:1072–1078. [PubMed: 20821542]
14. Guo X, Dong S, Petersen EJ, Gao S, Huang Q, Mao L. Biological Uptake and Depuration of Radio-labeled Graphene by *Daphnia magna*. *Environ. Sci. Technol*. 2013; 47:12524–12531. [PubMed: 24099417]
15. Oberdorster E, Zhu SQ, Blickley TM, McClellan-Green P, Haasch ML. Ecotoxicology of carbon-based engineered nanoparticles: Effects of fullerene (C-60) on aquatic organisms. *Carbon*. 2006; 44:1112–1120.
16. Henry TB, Menn F, Fleming JT, Wilgus J, Compton RN, Saylor GS. Attributing effects of aqueous C-60 nano-aggregates to tetrahydrofuran decomposition products in larval zebrafish by assessment of gene expression. *Environ. Health Perspect*. 2007; 115:1059–1065. [PubMed: 17637923]
17. Kim K, Jang M, Kim J, Kim SD. Effect of preparation methods on toxicity of fullerene water suspensions to Japanese medaka embryos. *Sci. Total Environ*. 2010; 408:5606–5612. [PubMed: 20723969]
18. Bensasson R, Bienvenue E, Dellinger M, Leach S, Setap P. C60 in Model Biological-Systems - a Visible-Uv Absorption Study of Solvent-Dependent Parameters and Solute Aggregation. *J. Phys. Chem*. 1994; 98:3492–3500.
19. OECD. Test guideline. Sediment-Water Chironomid Life-Cycle Toxicity Test Using Spiked Water or Spiked Sediment. 2009
20. OECD. Quideline for Testing of Chemicals 218. Sediment-Water Chironomid Toxicity Test using spiked Sediment. 2004
21. Ristola T, Pellinen J, Ruokolainen M, Kostamo A, Kukkonen J. Effect of sediment type, feeding level, and larval density on growth and development of a midge (*Chironomus riparius*). *Environmental Toxicology and Chemistry*. 1999; 18:756–764.
22. Ellis, AN.; Grant, M. Cytochemical Localization of H₂O₂ in Biological Tissues. In: Armstrong, D., editor. *Method in Molecular Biology*. Humana Press Inc.; 2002. p. 3
23. Bestwick C, Brown I, Bennett M, Mansfield J. Localization of hydrogen peroxide accumulation during the hypersensitive reaction of lettuce cells to *Pseudomonas syringae* pv *phaseolicola*. *Plant Cell*. 1997; 9:209–221. [PubMed: 9061952]
24. Droge W. Oxidative stress and aging. *Adv. Exp. Med. Biol*. 2003; 543:191–200. [PubMed: 14713123]
25. Khachadourian A, Maysinger D. Lipid Droplets: Their Role in Nanoparticle-induced Oxidative Stress. *Molecular Pharmaceutics*. 2009; 6:1125–1137. [PubMed: 19445477]
26. Hartmann NB, Buendia IM, Bak J, Baun A. Degradability of aged aquatic suspensions of C60 nanoparticles. *Environmental Pollution*. 2011; 159:3134–3137. [PubMed: 21684641]
27. Avanasi R, Jackson WA, Sherwin B, Mudge JF, Anderson TA. C60 Fullerene Soil Sorption, Biodegradation, and Plant Uptake. *Environ. Sci. Technol*. 2014; 48:2792–2797. [PubMed: 24521447]
28. Parks AN, Chandler GT, Ho KT, Burgess RM, Ferguson PL. Environmental biodegradability of [C¹⁴] single-walled carbon nanotubes by *Trametes versicolor* and natural microbial cultures found in New Bedford Harbor sediment and aerated wastewater treatment plant sludge. *Environ. Toxicol. Chem*. 2015; 34:247–251. [PubMed: 25352477]
29. Zhang L, Petersen EJ, Habteselassie MY, Mao L, Huang Q. Degradation of multiwall carbon nanotubes by bacteria. *Environmental Pollution*. 2013; 181:335–339. [PubMed: 23859846]
30. Wang J, Wages M, Yu S, Maul JD, Mayer G, Hope-Weeks L, Cobb GP. Bioaccumulation of Fullerene (C-60) and Corresponding Catalase Elevation in *Lumbriculus Variegatus*. *Environmental Toxicology and Chemistry*. 2014; 33:1135–1141. [PubMed: 24477927]
31. Chiou C, Freed V, Schmedding D, Kohnert R. Partition-Coefficient and Bioaccumulation of Selected Organic Chemicals. *Environ. Sci. Technol*. 1977; 11:475–478.
32. Mackay D, Fraser A. Bioaccumulation of persistent organic chemicals: mechanisms and models. *Environmental Pollution*. 2000; 110:375–391. [PubMed: 15092817]

33. Petersen EJ, Akkanen J, Kukkonen JVK, Weber WJ Jr. Biological Uptake and Depuration of Carbon Nano-tubes by *Daphnia magna*. *Environ. Sci. Technol.* 2009; 43:2969–2975. [PubMed: 19475979]
34. Petersen EJ, Pinto RA, Mai DJ, Landrum PF, Weber WJ Jr. Influence of Polyethyleneimine Graftings of Multi-Walled Carbon Nanotubes on their Accumulation and Elimination by and Toxicity to *Daphnia magna*. *Environ. Sci. Technol.* 2011; 45:1133–1138. [PubMed: 21182278]
35. Collins R, Harmon B, Gobe G, Kerr J. Internucleosomal Dna Cleavage should Not be the Sole Criterion for Identifying Apoptosis. *Int. J. Radiat. Biol.* 1992; 61:451–453. [PubMed: 1349327]
36. Buja L, Eigenbrodt M, Eigenbrodt E. Apoptosis and Necrosis - Basic Types and Mechanisms of Cell-Death. *Arch. Pathol. Lab. Med.* 1993; 117:1208–1214. [PubMed: 8250690]
37. Lebrecht D, Geist A, Ketelsen U, Haberstroh J, Setzer B, Walker UA. Dexrazoxane prevents doxorubicin-induced long-term cardiotoxicity and protects myocardial mitochondria from genetic and functional lesions in rats. *Br. J. Pharmacol.* 2007; 151:771–778. [PubMed: 17519947]
38. Kobashigawa S, Kashino G, Suzuki K, Yamashita S, Mori H. Ionizing radiation-induced cell death is partly caused by increase of mitochondrial reactive oxygen species in normal human fibroblast cells. *Radiat Res.* 2015; 183:455–464. [PubMed: 25807320]
39. Ineichen H, Riesenwilli U, Fisher J. Experimental Contributions to the Ecology of Chironomus (Diptera).2. Influence of the Photoperiod on the Development of Chironomus-Plumosus in the 4th Larval Instar. *Oecologia.* 1979; 39:161–183.
40. Liber K, Call D, Dawson T, Whiteman F, Dillon T. Effects of Chironomus tentans larval growth retardation on adult emergence and ovipositing success: Implications for interpreting freshwater sediment bioassays. *Hydrobiologia.* 1996; 323:155–167.
41. Nair PMG, Park SY, Choi J. Evaluation of the effect of silver nanoparticles and silver ions using stress responsive gene expression in Chironomus riparius. *Chemosphere.* 2013; 92:592–599. [PubMed: 23664472]

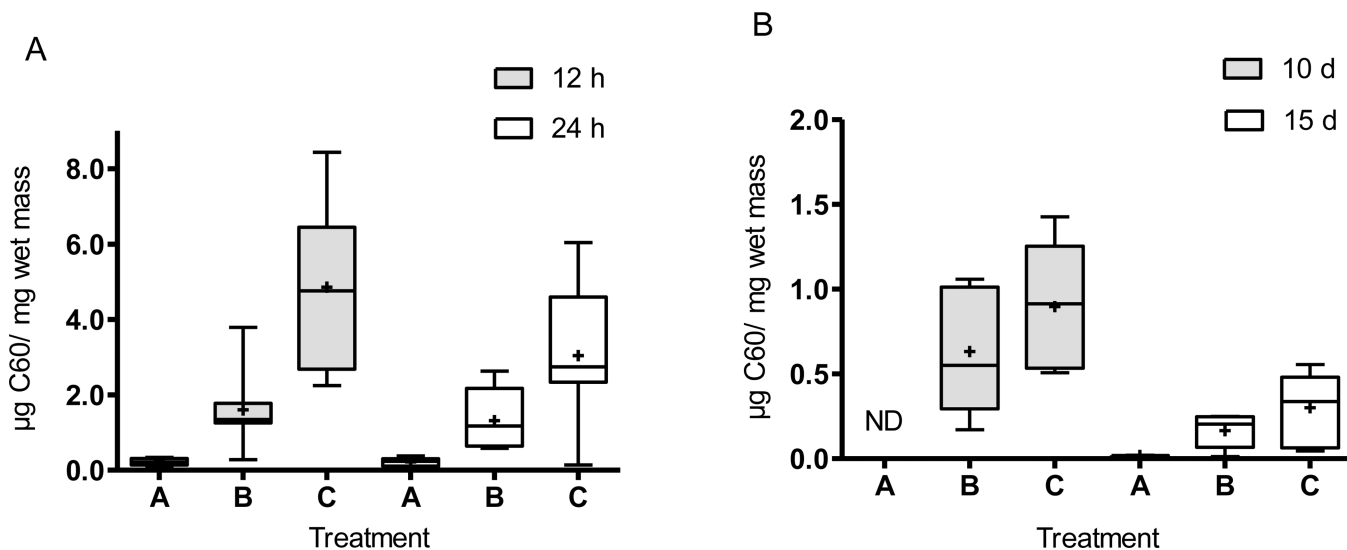


Fig. 1. Box plots of the results for larval larvae body burdens after (A) acute (n = 6 in treatment A for both time points; for treatments B, C, n = 7 for both time points) and (B) chronic exposures (treatments B, C n = 5 after 10 d; and B and C n = 5 and 6 after 15 d, respectively while n=2 for treatment A after 15 d) to different treatments of C₆₀. The symbol “+” indicates mean values, and whiskers indicate minimum and maximum values and bars indicate quartile ranges. Asterisks indicate significant differences from controls. ND = not detectable.

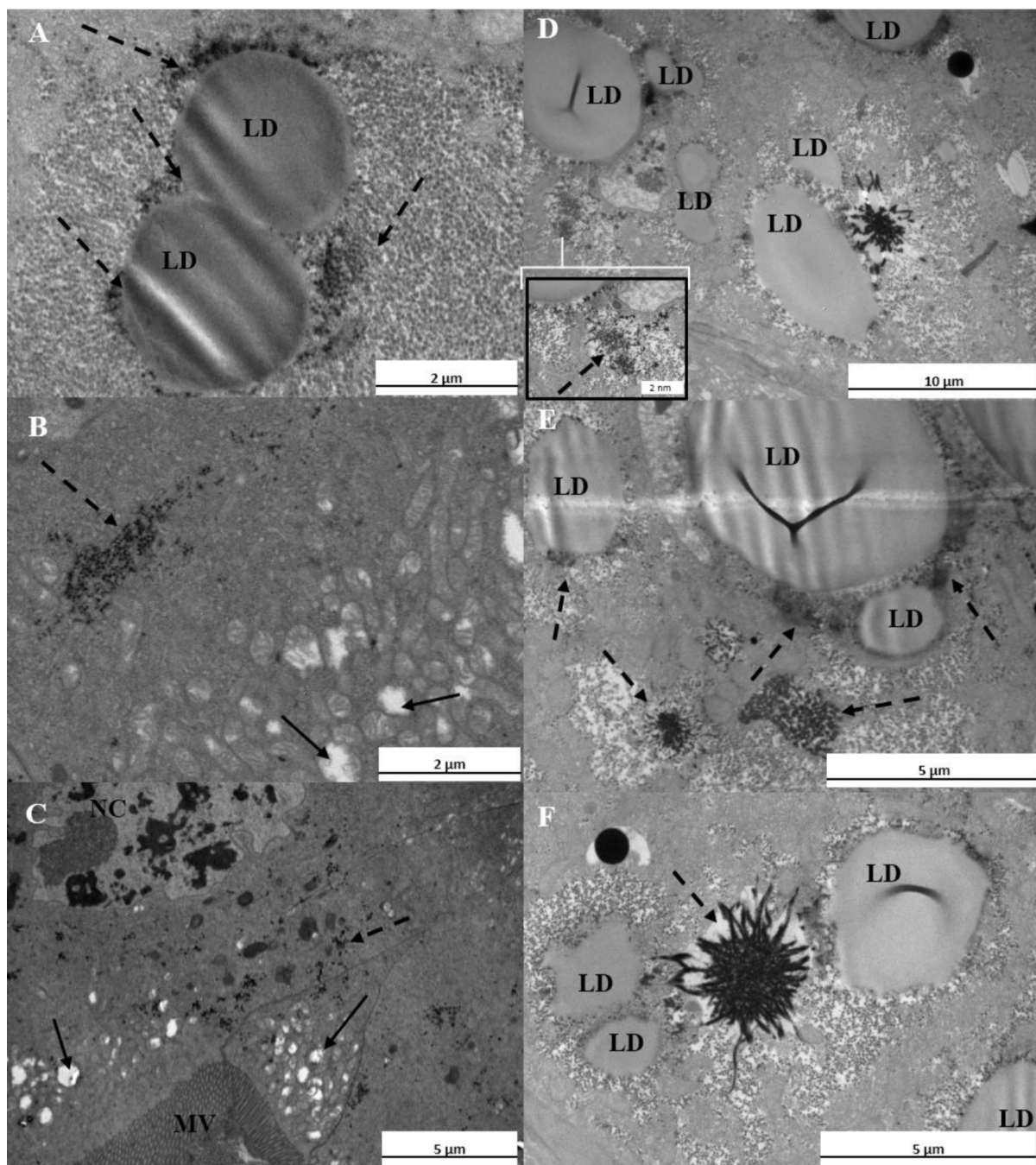


Fig. 2.
 A–F. Transmission electron micrographs of *C. riparius* after 10 d of exposure in treatment A. The symbols MV, LD and NC indicate microvilli layer, lipid droplet and nucleus, respectively. Solid arrows indicate mitochondria, while dashed arrows indicate precipitates. (A) Lipid droplets and precipitates between them. (B) Precipitates in the tissue and swollen mitochondria (C) The structure of the nucleus, swollen mitochondria and precipitates next to the microvilli layer. (D) Lipid droplets and precipitates located near of them; in the inserted

Figure is a higher magnification of the precipitate. (E) Large precipitates close to lipid droplets. (F) Lipid droplets and large precipitate between them.

NIST Author Manuscript

NIST Author Manuscript

NIST Author Manuscript

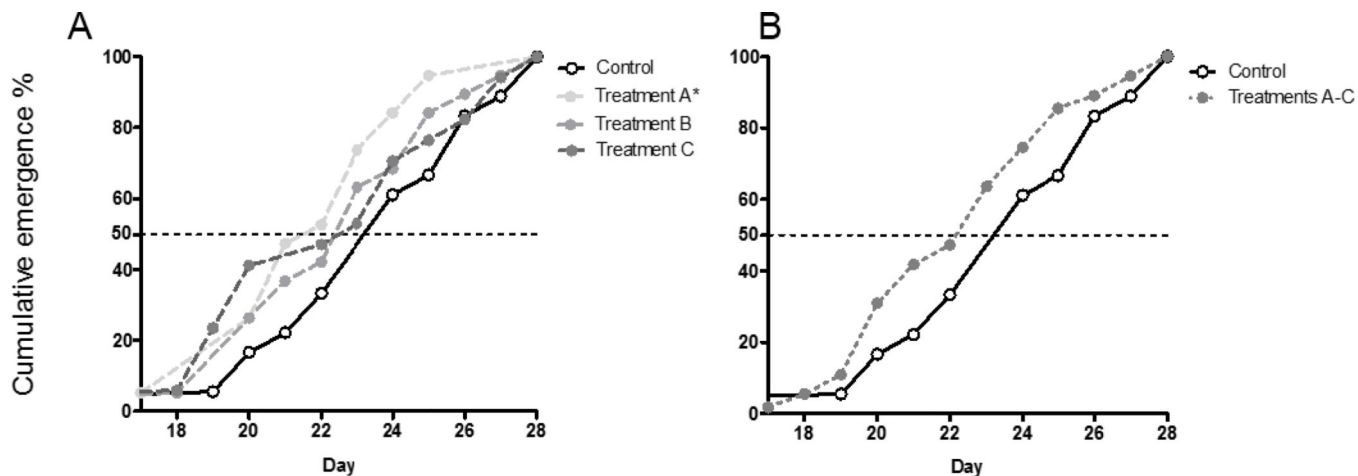


Fig. 3. Cumulative emergence (%) of the midges exposed to thin fullerenes layers on the top of the sediment. A) Results analyzed separately (n=18, 19, 19, 17, respectively) B) Results where all fullerene treatments (A, B, and C) are combined. Asterisks indicate significant differences from controls. (n=18 and 55, respectively). Treatments were compared to the control using the Log-rank Mantel-Cox test. The significant difference ($p < 0.05$) for Treatment A compared to the control is indicated by an asterisk.

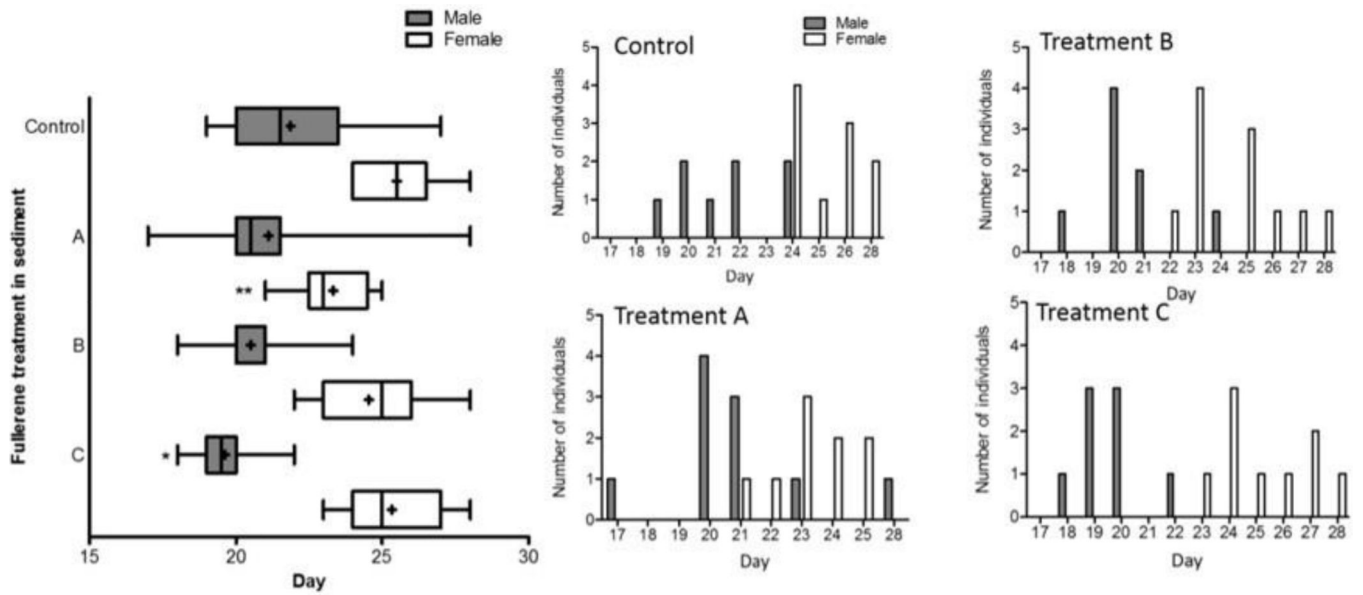


Fig.4. Emergence day of the females and males for the control treatment and treatments A, B, and C (n=18, 19, 19, 17, respectively). Histogram figures show the differences in emergence time between treatments. The symbol “+” indicates mean values, and whiskers indicate minimum and maximum values. Asterisks indicate significant differences from controls (Log-rank Mantel-Cox test, * p < 0.05)

Table 1

The quantity of settled fullerenes on top of the sediment for each treatment in mg/cm² (mean ± standard deviations; n = 3 (treatment A) or 5 (treatments B and C) samples taken from individual replicate beakers for treatments B and C or the stock suspension for treatment A).

	BODY BURDEN & OXIDATIVE STRESS			DEVELOPMENTAL EFFECTS		
	Acute exposure		Chronic exposure		Growth exposure	Emergence exposure
	Uptake	TEM	Uptake	TEM		
Treatment A	0.031 (± 0.001)		0.023(± 0.003)		0.031 (± 0.001)	0.028 (± 0.001)
Treatment B	0.211 (± 0.001)		0.181 (± 0.001)		0.180 (± 0.06)	0.210 (± 0.01)
Treatment C	0.560 (± 0.003)	0.480 (± 0.001)	0.480 (± 0.01)	0.490 (± 0.004)	Previously tested,[7] not analyzed in this study	0.540 (± 0.12)

Table 2

Summary of results for *C. riparius* experiments.

UPTAKE							
LOCALIZATION OF OXIDATIVE STRESS							
Treatment	Acute exposure	Chronic exposure	Acute Exposure	Chronic exposure			
Positive Control	12 h	24 h	10 d	15 d	12 h	10 d	large precipitates localized between lipid droplets and under microvilli layer, increase number of lipid droplets
Average amount of extracted fullerene in larvae (µg/mg wet mass)							
A	0.22 ± 0.10	0.22 ± 0.11	---	0.01	minor precipitates, localized under microvilli layer	large precipitates localized between lipid droplets and under microvilli layer	
	1.60 ± 1.07	1.31 ± 0.80	0.46 ± 0.25	0.10 ± 0.06	large precipitates localized between lipid droplets and under microvilli layer	large precipitates localized between lipid droplets and under microvilli layer	
B	4.85 ± 2.26	3.04 ± 1.85	0.69 ± 0.31	0.19 ± 0.13	some precipitates, localized under microvilli layer	large precipitates localized between lipid droplets and under microvilli layer	
	DEVELOPMENT						
C	8.82 ± 1.42	8.94 ± 1.89	9.08 ± 1.42	9	24	21.5/25.5	
	2.26	1.85	0.31	0.13	22	20.5/23	
C	2.26	1.85	0.31	0.13	23	20/25	
	2.26	1.85	0.31	0.13	23	19.5/25	